Intrinsic Gap States in Semiconductor Nanocrystals

Peter C. Sercel
Department of Physics, University of Oregon, Eugene, Oregon 97403

Al. L. Efros and M. Rosen
Nanostructure Optics Section, Naval Research Laboratory, Washington, D.C. 20375

(Received 16 April 1999)

We demonstrate the existence of *intrinsic* gap states in bare and capped semiconductor nanocrystals within multiband effective mass theory. These states originate from Shockley-like surface states which, in small nanocrystals, extend over the entire crystal volume, facilitating their observation in absorption as well as in photoluminescence. The conditions under which such intrinsic states might be observed are discussed in light of the theory developed and analysis of the band parameters of direct gap semiconductors.

PACS numbers: 73.20.Dx, 71.24.+q, 78.66.–w

The optical properties of nanosize semiconductor crystals have attracted much attention because of their potential applications and their fundamental interest [1–3]. Their optical properties usually arise from transitions between the quantum size levels of the conduction bands (CB) and valence bands (VB). We describe a new class of *intrinsic* nanocrystal (NC) states within the multiband effective mass approximation whose energy is size dependent and which lie between the bulk conduction and valence band edges—they are *intrinsic* gap states (GS). By intrinsic we mean that these states are not associated with point defects such as impurities, or with surface dangling bonds, but rather occur in NCs with perfectly passivated surfaces or interfaces as in Shockley's model of surface states [4]. These electronic states could play an important role in the photoabsorption and photoluminescence (PL) of NCs. Similar types of intrinsic gap states, i.e., whose energy depends on the bulk properties of the semiconductors, have been experimentally observed in the energy spectra of optical phonons [5] and excitons [6] in semiconductor NCs (so-called surface phonons and surface excitons). Electronic gap states of the type we describe have not yet been observed experimentally; in this paper we analyze the conditions under which they might be found.

The conditions for the existence of an intrinsic GS are intimately connected with the character of the surface (for the case of bare NCs) or the heterointerface (for the case of capped NCs). In the effective mass approximation, interfaces are characterized through boundary conditions (BCs). While the choice of BCs within effective mass theory is somewhat arbitrary, general BCs have been developed for planar heterointerfaces [7], but more commonly the wave function and the normal component of the probability current are required to be continuous ("conventional" BCs) [7,8]. Zhu and Kroemer, however, using a tight-binding approximation, showed that, generally, the conventional matching conditions at a planar heterointerface should be modified by inclusion of an interface delta-function potential, which under certain conditions can give rise to interface states. Only for so-called "normal" heterojunctions, where the interface transfer matrix element equals the geometric mean of the nearest-neighbor transfer matrix elements associated with the two respective bulk semiconductors, do the conventional BCs apply [9].

In this paper we present a theoretical study of intrinsic gap states in bare and capped spherical NCs of zinc blende semiconductors. Using the eight-band Pidgeon and Brown model (PB) [10] to describe the Hamiltonian of the bulk material, we demonstrate that the use *even of conventional BCs* leads to three distinct types of intrinsic GSs within the effective mass approximation. The first two arise in heterostructure NCs with abrupt changes in the energy band parameters across the interface, while the third may exist in bare NCs of specific materials, e.g., InP or CdS.

The PB model simultaneously takes the coupling of the conduction and valence bands into account exactly and the contribution of remote bands to the effective masses of the electrons and holes in second-order perturbation theory. This model successfully describes the complex band structure around the Γ point of the Brillouin zone of semiconductors having cubic lattice symmetry. In the limit of zero spin-orbit coupling, $\Delta = 0$, and assuming spherical symmetry, this Hamiltonian is represented in the Bloch function basis $|S\rangle$, $|X\rangle$, $|Y\rangle$, $|Z\rangle$ as

$$\hat{H}_{\mathrm{PB}} = \frac{\hbar^2}{2m_o}\begin{pmatrix} \varepsilon_g + \alpha\hat{k}^2 & iP\hat{k}_x & iP\hat{k}_y & iP\hat{k}_z \\ -iP\hat{k}_x & -\beta_l\hat{k}_x^2 - \beta_h\hat{k}_{\perp x}^2 & -6\gamma\hat{k}_x\hat{k}_y & -6\gamma\hat{k}_x\hat{k}_z \\ -iP\hat{k}_y & -6\gamma\hat{k}_x\hat{k}_y & -\beta_l\hat{k}_y^2 - \beta_h\hat{k}_{\perp y}^2 & -6\gamma\hat{k}_y\hat{k}_z \\ -iP\hat{k}_z & -6\gamma\hat{k}_x\hat{k}_z & -6\gamma\hat{k}_y\hat{k}_z & -\beta_l\hat{k}_z^2 - \beta_h\hat{k}_{\perp z}^2 \end{pmatrix}. \quad (1)$$

 0031-9007/99/83(12)/2394(4)$15.00

Here, $\hat{k}_{x,y,x} = -i\partial/\partial_{x,y,z}$, $\hat{k}^2_{\perp,i} = \hat{k}^2 - \hat{k}^2_i$, $P = -2i\langle S|\hat{p}_z|Z\rangle/\hbar$, $E_g = \hbar^2\varepsilon_g/2m_0$ is the energy gap, $\beta_l = \gamma_1 + 4\gamma$, and $\beta_h = \gamma_1 - 2\gamma$ are the contribution of remote bands to the effective masses of the light and heavy holes, written in terms of "modified" Luttinger parameters $\gamma_1 = \gamma_1^L - E_p/3E_g$, $\gamma = \gamma^L - E_p/6E_g$, where $E_p = \hbar^2P^2/2m_0$ [10]. The inverse of the electron effective mass, m_c, at the bottom of the conduction band can be expressed $m_c^{-1} = m_0^{-1}(\alpha + E_p/E_g)$.

In this approach, each electron and hole state in spherical NCs is characterized by its parity and total angular momentum $\mathbf{F} = \mathbf{J} + \mathbf{L}$, where $\mathbf{J}$ is the Bloch band-edge angular momentum (0 for the conduction band; 1 for the valence bands) and $\mathbf{L}$ is the envelope angular momentum. The corresponding wave functions can be expressed [11]

$$\Psi_{F,F_z}(\mathbf{r}) = \sum_{J,L} R_L^{F,J}(r)\,|F, F_z; J, L\rangle, \tag{2}$$

where $|F, F_z; J, L\rangle$ are eigenstates of the total angular momentum [11]. With the spherical PB Hamiltonian, we then obtain two sets (one for each parity) of second-order differential equations for the radial functions $R_L^{F,J}(r)$:

$$\begin{aligned}
&[\varepsilon_g - \varepsilon - \alpha\Delta_F]R_F^{F,0} - a_F^- PA_{F-1}^+ R_{F-1}^{F,1} - a_F^+ PA_{F+1}^- R_{F+1}^{F,1} = 0,\\
&-a_F^- PA_F^- R_F^{F,0} + (D_F^- - \varepsilon)R_{F-1}^{F,1} - b_F\gamma A_{F+1}^{-2} R_{F+1}^{F,1} = 0,\\
&-a_F^+ PA_F^+ R_F^{F,0} - b_F\gamma A_{F-1}^{+2} R_{F-1}^{F,1} + (D_F^+ - \varepsilon)R_{F+1}^{F,1} = 0,
\end{aligned} \tag{3}$$

where $a_F^{\pm} = \sqrt{(1 \pm \delta_F)/2}$, $b_F = 3\sqrt{1 - \delta_F^2}$, $c_F^{\pm} = 1 \pm 3\delta_F$, and $\delta_F = 1/(2F + 1)$, the raising and lowering operators $A_l^+ = -\frac{\partial}{\partial r} + \frac{l}{r}$, $A_l^- = \frac{\partial}{\partial r} + \frac{l+1}{r}$, and the radial Laplacian $\Delta_l = \frac{\partial^2}{\partial^2 r} + \frac{2}{r}\frac{\partial}{\partial r} - \frac{l(l+1)}{r^2}$, $D_F^{\pm} = (\gamma_1 + c_F^{\pm}\gamma)\Delta_{F\pm1}$, and $A_l^{\pm 2} = A_{l\pm1}^{\pm} A_l^{\pm}$. This equation is valid for $F \geq 0$. The second equation,

$$[(\gamma_1 - 2\gamma)\Delta_F - \varepsilon]R_F^{F,1} = 0, \tag{4}$$

is valid for $F \geq 1$.

Equations (3) and (4) were derived for a homogeneous semiconductor. In heterostructures with abrupt heterointerfaces, a general solution to Eqs. (3) and (4) can be found in each homogeneous region separately and the total wave function determined by imposing appropriate BCs. In spherical NCs, the simplest form of the conventional BCs reduces to continuity of each component, $R_L^{F,J}$, of the radial envelope wave function, Eq. (2), and continuity of the normal component of the velocity at the heterointerface:

$$(\mathbf{n}\cdot\hat{\mathbf{V}})\Psi_{F,F_z}(\mathbf{r})|_{r=a^-} = (\mathbf{n}\cdot\hat{\mathbf{V}})\Psi_{F,F_z}(\mathbf{r})|_{r=a^+}, \tag{5}$$

where $\mathbf{n} = \mathbf{r}/r$ and $\hat{\mathbf{V}} = \frac{1}{\hbar}\nabla_{\mathbf{k}}\hat{H}(\mathbf{k})$. The radial velocity operator may be represented in a basis of eigenstates of total angular momentum, $|F, F_z; J, L\rangle$, by using the familiar rules for angular momentum addition and integrating over angular variables. For the states corresponding to Eq. (3),

$$(\mathbf{n}\cdot\hat{\mathbf{V}})\Psi_{F,F_z}(\mathbf{r}) = 2i\begin{pmatrix} -\alpha\delta_r R_F^{F,0} + a_F^- \frac{P}{2} R_{F-1}^{F,1} - a_F^+ \frac{P}{2} R_{F+1}^{F,1} \\ -a_F^- \frac{P}{2} R_F^{F,0} + B_F^- R_{F-1}^{F,1} - b_F\gamma A_{F+1}^- R_{F+1}^{F,1} \\ a_F^+ \frac{P}{2} R_F^{F,0} + b_F\gamma A_{F-1}^+ R_{F-1}^{F,1} + B_F^+ R_{F+1}^{F,1} \end{pmatrix}, \tag{6}$$

where $B_F^{\pm} = (\gamma_1 - 2c_F^{\pm}\gamma)\delta_r + \frac{3}{2}c_F^{\pm}\gamma(A_{F\pm1}^- - A_{F\pm1}^+)$. Each component of this array is required to be continuous at the heterointerface. For the other parity the equation for the normal component of the velocity is

$$\frac{(\mathbf{n}\cdot\hat{\mathbf{V}})\Psi_{F,F_z}(\mathbf{r})}{2i} = \left[(\gamma_1 - 2\gamma)\frac{\partial}{\partial r} - 3\frac{\gamma}{r}\right]R_F^{F,1}. \tag{7}$$

Together, Eqs. (3), (4), (6), and (7) completely describe the electronic structure of quantum size levels in spherical NCs within the eight-band effective mass model. We will now show three cases where GSs exist as solutions of these equations. We begin with the simplest case of the single-component heavy-hole states in capped NCs, which are described by Eqs. (4) and (7). Analysis of these equations shows that GSs exist for sufficiently large discontinuity in the parameter γ across the interointerface at $r = a$:

$$\beta_h^i \frac{\partial_r R_F^{F,1}}{R_F^{F,1}}\bigg|_{r=a^-} - \beta_h^o \frac{\partial_r R_F^{F,1}}{R_F^{F,1}}\bigg|_{r=a^+} = 3\frac{\gamma^i - \gamma^o}{a}. \tag{8}$$

The right side of this equation, which represents a discontinuity in the mass-weighted normal derivatives of the radial wave functions, can be interpreted as the effect of an attractive delta-function potential at the interface (see Ref. [9]) which arises from terms of d symmetry in the Hamiltonian, Eq. (1). In the present context, the strength of the potential is proportional to $\gamma^i - \gamma^o$ and inversely proportional to the NC radius, leading to GSs in finite size NCs if $\gamma^i > \gamma^o$. This situation is exemplified by CdS NCs embedded in HgS (Fig. 1). This system constitutes an "antidot" since the band gap of the CdS core exceeds that of the HgS matrix in which it is embedded. The size dependence of the $F = 1$ level, calculated using the parameters of Ref. [12], is shown for this system in Fig. 1. The state starts from the top of the valence band of HgS for large CdS antidot core radii and enters the gap as the core radius decreases. The wave functions decay evanescently from the interface [see Fig. 1(b)], exhibiting a cusp which is connected with the discontinuity of the radial derivatives, a feature which is essential for the existence of GSs.

Analysis of Eqs. (3) and (6) shows that GSs usually do not exist in capped NCs described by the conventional BCs because the effective mass parameters for the constituent materials in standard heterojunctions are close to

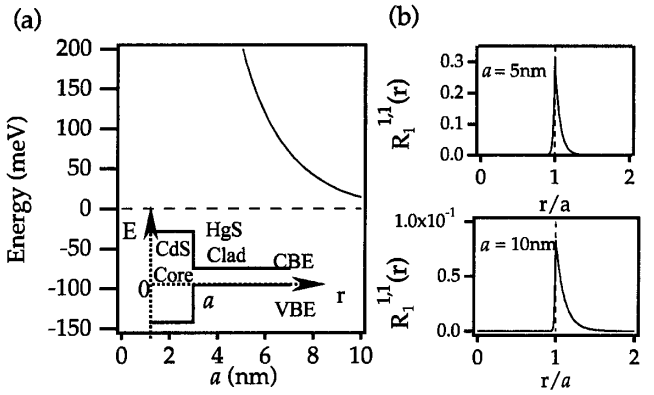

FIG. 1. Pure heavy-hole gap state in antidot CdS/HgS NCs: (a) size dependence of the energy for the $F = 1$ state. Inset: schematic of the band diagram (E_g for HgS is taken to be 200 meV following Ref. [13]); (b) size dependence of the radial wave function in antidots with radii, a, of 5 and 10 nm.

each other. However, for some heterojunction systems the parameters α, β have opposite signs across the heterointerface. As a result, in these systems the radial derivatives must have opposite signs across the heterointerface, consequently leading to a cusp in the wave function and thus the possibility of a second type of GS. However, these states are highly localized near the heterointerface; thus these results are outside the range where the effective mass approximation can be applied. A quantitative treatment of these states would require analysis within *ab initio* atomistic models.

A third type of GS, which emerges from the coupling between the conduction and valence bands, can exist in bare NCs within the effective mass model. In bare NCs, the surface is conventionally described by an infinite barrier. Description of these states proceeds from Eq. (3) with the BC that all components of the radial wave function vanish at the NC surface, $r = a$. The resulting dispersion relation which describes the size dependence of the energy levels has the form [13]

$$j_{F+1}(k_-a)j_{F-1}(k_ha) + \tfrac{F}{F+1}j_{F+1}(k_ha)j_{F-1}(k_-a) = \tfrac{\alpha}{|\alpha|}\sqrt{\tfrac{\alpha}{\beta_l}}\,\tfrac{\varepsilon+\beta_l k_-^2}{Pk_-}\,j_F(k_-a)\left[j_{F-1}(k_ha) - \tfrac{Fj_{F+1}(k_ha)}{F+1}\right], \qquad (9)$$

where $k_h^2 = \varepsilon/\beta_h$ and $k_-^2 \approx \varepsilon(\varepsilon - \varepsilon_g)/P^2$. Equation (9) describes the quantum size levels in the conduction band, when $\varepsilon > \varepsilon_g$, and in the valence band, when $\varepsilon < 0$. However, they also have solutions when the energy $0 < \varepsilon < \varepsilon_g$. In this case k_-^2 and k_h^2 are negative, corresponding to evanescently decaying wave functions.

It is easy to find solutions for these equations in the limit of large radius a where $|k_-|a \gg 1$, $|k_h|a \gg 1$. In this case, using asymptotic expressions for the spherical Bessel functions of imaginary argument, Eq. (9) becomes

$$1 = -\frac{\alpha}{|\alpha|}\sqrt{\frac{\alpha}{\beta_l}}\,\frac{\varepsilon + \beta_l k_-^2}{P|k_-|}. \qquad (10)$$

This equation has solutions only if the contribution of remote bands to the electron and hole effective masses are both negative: $\alpha < 0$, $\beta_l < 0$. For large a, the GS energy $\varepsilon_s = \beta_l\varepsilon_g/(\beta_l + \alpha)$ is independent of the angular momentum F.

InP is one material which satisfies this condition. The size dependence of the resulting intrinsic GSs, calculated for different angular momenta, F, is shown in Fig. 2(a) together with the size dependence of the lowest hole and electron levels. Calculations were done for InP NCs with $E_g = 1.424$ eV, $E_p = 20.6$ eV, $\alpha = -1.2$, $\gamma_1 = 0.41$, and $\gamma = -0.51$ [14], and assuming $\Delta = 0$. All GSs start from the same energy ε_s at large radii and fan out into the band gap with decreasing size according to their particular angular momenta. In Fig. 2(b) we show the size dependence of the radial wave functions of the $F = 1$ GS for NCs with radii 8, 4, and 2 nm, whose energy is approximately the same. In large NCs the GS is localized near the surface while it becomes increasingly extended over the entire internal volume of the NC with decreasing NC radius. However, these radial wave functions decay to zero near the surface within a length on the order of the unit cell. This is because the wave functions contain appreciable admixture of the complex "wing-band" components with wave vector modulus $\sim P^2/\alpha\beta$, lying outside the first Brillouin zone, and which consequently do not describe physical states as discussed in Ref. [15]. As shown in Refs. [13,15], the contribution of these wing-band states can be removed by taking the limit $\alpha, \beta \to 0$, which results in a modified boundary condition in which the wave

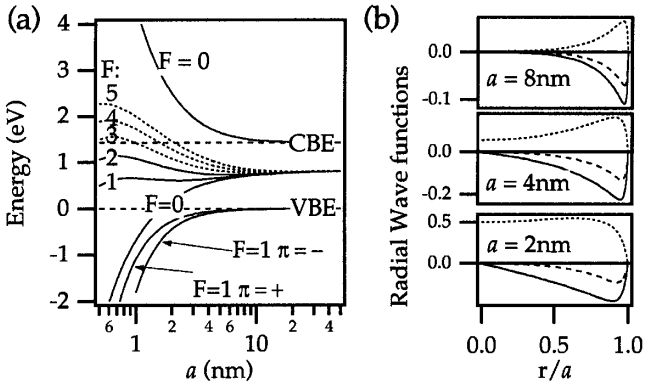

FIG. 2. GSs in bare InP NCs. (a) Size dependence of the gap states with various angular momenta ($F = 0, \ldots, 5$) and the lowest quantum levels in the conduction ($F = 0$) and valence ($F = 1$, parity $\pi = \pm 1$) bands. The band states as well as GSs which are active in band-edge transitions are indicated by solid lines while other GSs are shown with dotted lines. (b) Size dependence of the radial $F = 1$ gap state wave functions: $R_0^{1,1}$, $R_2^{1,1}$, and $R_1^{1,0}$ are indicated by dotted, dashed, and solid lines, respectively, for three different size NCs.

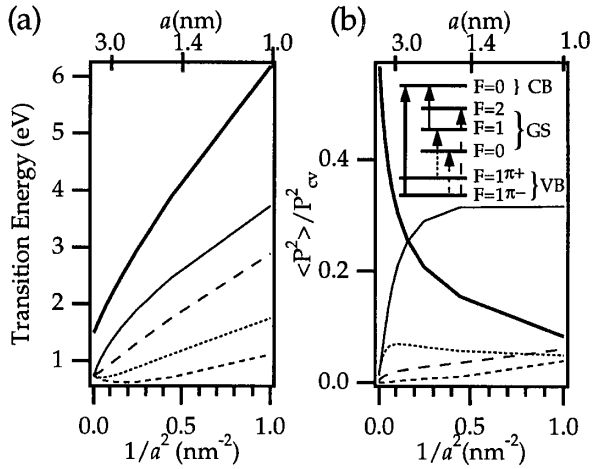

FIG. 3. The size dependence of the transition energy (a) and average squared transition dipole (b) of the band edge and GS transitions. In (b) the transition dipole is plotted in units of the interband matrix element $P_{cv}^2 = |\langle s|\hat{p}_z|z\rangle|^2$. The inset shows a schematic of the optically allowed transitions. The bold line describes the lowest energy band-to-band transition; the plain solid line indicates the transition between the CB and the $F = 1$ GS; the dashed and dotted lines correspond to transitions between GSs and the VB as identified in the schematic.

function is not required to vanish at the NC surface [13]. Consequently, until a more rigorous procedure for handling the NC surface is developed, the present description of these states must be regarded cautiously.

An important question therefore is: How would such states manifest themselves experimentally? Figure 3 shows the size dependence of the energy (a) and oscillator strengths (b) of the dipole allowed transitions ($\Delta F = 0, \pm 1$) between the lowest energy electron and hole quantum size levels and gap states in InP NCs (see inset). The bold line describes the band-to-band transition. The thin solid line corresponds to the transition from the $F = 1$ GS to the CB. The transition dipole element of this transition is larger than that of the band-to-band transition in small NCs, which would make this transition active even in absorption measurements. The transitions between the GSs and the hole levels (dashed and dotted lines) are much weaker. As a result, it is possible that the absorption band edge and PL in small NCs could be determined by GS-CB quantum size level transitions.

Analysis of the band parameters shows that this type of intrinsic GS may occur in bare InP or CdS NCs. Bare CdS NCs do show deep lines in their PL [16] which were interpreted as deep impurity transitions to the CB. In InP, the existence of a dipole-allowed transition between the $F = 1$ GS and the lowest $1S$ electron state may explain the lack of success in describing the PL excitation (PLE) spectra of this material using the standard scheme of transitions between the quantum size levels of the CB and VB [19] (which successfully describes the PLE spectra of CdSe [17] and InAs [18]). However, even within the limitations of the present model the GS transitions calculated lie in the approximate range of the experimentally measured absorption edge transitions seen in bare InP NCs [19]. It may also explain the recent observation of upconverted PL in this material [20].

In summary, we have shown the existence of *intrinsic* GSs in semiconductor NCs within the effective mass theory. These states do not usually occur in capped NCs with similar material parameters across the heterointerface. However, we found that even conventional BCs give us GSs in two cases: in antidot-type CdS NCs embedded in HgS and in bare NCs where the contribution of remote bands to the conduction and valence band effective masses is negative, as exemplified by InP and CdS NCs.

This material is based upon work supported by the U.S. Army Research Office under Grant No. DAAH04-96-1-0091 and by the Office of Naval Research.

[1] S. Schmitt-Rink, D. A. B. Miller, and D. S. Chemla, Phys. Rev. B **35**, 8113 (1987).
[2] L. E. Brus, Appl. Phys. A **53**, 465 (1991).
[3] A. P. Alivisatos, Science **271**, 933 (1996).
[4] S. G. Davison and M. Steslicka, *Basic Theory of Surface States* (Clarendon Press, Oxford, 1992).
[5] S. Hayashi and H. Kanamori, Phys. Rev. B **26**, 7079 (1982).
[6] A. I. Ekimov *et al.,* Sov. Phys. JETP **83**, 1054 (1986).
[7] M. V. Kisin, B. L. Gelmont, and S. Luryi, Phys. Rev. B **58**, 4605 (1998).
[8] E. I. Ivchenko and G. Pikus, *Superlattices and Other Heterostructure,* Springer Series in Solid State Science Vol. 110 (Springer, Berlin, 1995).
[9] Q.-G. Zhu and H. Kroemer, Phys. Rev. B **27**, 3519 (1983).
[10] C. R. Pidgeon and R. N. Brown, Phys. Rev. **146**, 575 (1966).
[11] Peter C. Sercel and Kerry J. Vahala, Phys. Rev. B **42**, 3690 (1990).
[12] W. Jaskolski and G. W. Bryant, Phys. Rev. B **57**, R4237 (1998).
[13] Al. L. Efros and M. Rosen, Phys. Rev. B **58**, 7120 (1998).
[14] S. I. Kokhanovskii *et al.,* Sov. Phys. Solid State **33**, 967 (1991).
[15] S. R. White and L. J. Sham, Phys. Rev. Lett. **47**, 879 (1981).
[16] A. I. Ekimov *et al.,* J. Lumin. **46**, 83 (1990).
[17] D. J. Norris and M. G. Bawendi, Phys. Rev. B **53**, 16 338 (1996).
[18] U. Banin *et al.,* J. Chem. Phys. **109**, 2306 (1998).
[19] D. Bertram, O. I. Micic, and A. J. Nozik, Phys. Rev. B **57**, R4265 (1998).
[20] E. Poles, D. C. Selmarten, O. Micic, and A. Nozik (to be published).